Supporting Information

Creation of Hollow Microtubular Iron Oxalate Dihydrate Induced by a Metallo-Supramolecular Micelle Based on the Self-assembly of Potassium Ferrioxalate and Sodium Dodecyl Sulphate

Yue Teng[a], Le Xin Song[*,a,b], Wei Liu[*,a], Juan Xia[a], Li Zhao[b], Qing Shan Wang[b], Mao Mao Ruan[b]

[a] *CAS Key Laboratory of Materials for Energy Conversion, Department of Materials Science and Engineering, University of Science and Technology of China, Jin Zhai Road 96, Hefei, China 230026*
[b] *Department of Chemistry, University of Science and Technology of China, Jin Zhai Road 96, Hefei, China 230026*
Email: solexin@ustc.edu.cn; wliu@ustc.edu.cn;
Fax: +86-551-63601592

A list of the contents for all the Supporting Information

Experimental Section

***Materials*:** Sodium dodecyl sulphate (SDS) and potassium ferrioxalate (PF) were obtained from Shanghai Chemical Reagent.

Synthesis of metallosurfactants of PF and SDS: 0.5 g PF was dissolved in 40 mL of H_2O at 298 K, and then 1.0 g of SDS was dissolved in the PF solution, generating a mixed solution of PF and SDS. A series of solutions composed of PF and SDS were also prepared using the same method but with different initial masses.

Hydrothermal experiments: A solution with 8.68×10^{-2} mol dm^{-3} SDS and 2.50×10^{-2} mol dm^{-3} PF was completely transferred into a 50 mL sealed stainless steel autoclave and heated to 473 K for 4 h. Fine blond tube-like crystals ($FeC_2O_4 \cdot 2H_2O$, 0.14 g, 76%) were collected by filtration, washed several times with distilled water and ethanol, and dried in vacuum. The synthesis is repeated but with other two concentrations, giving either a reddish-brown powder for 8.68×10^{-3} mol dm^{-3} SDS or no precipitation for 5.0×10^{-3} mol dm^{-3} PF.

Characterization: Field emission scanning electron microscopy (FESEM, Supra 40) has been used to produce the structural information. In addition, the crystallinity of the samples was determined by the powder X-ray diffraction pattern (XRD) (Philips X'Pert Pro X-ray diffractometer) using a monochromatized Cu Kα radiation source (40 kV, 40 mA) with a wavelength of 0.1542 nm and analyzed in the range $10° \leq 2\theta \leq 80°$. Thermogravimetry and derivative thermogravimetry (TG/DTG) measurements were determined on a TGA-50 thermogravimetric analyzer at a constant heating rate of 10.0 K min^{-1} in air. The hydrodynamic radius of the micelles was obtained on a DynaPro-MS800 dynamic light scattering (DLS) instrument (Protein Solution, Lakewood, NJ) equipped with a thermostatic sample chamber.

Conductivity measurements: A Leici DDSJ-308 conductivity meter with automatic temperature compensation and automatic calibration was used to record the conductivity of solutions at 298 K. A conductance cell with a cell constant of 0.984 cm^{-1} was used in a water bath whose temperature was kept at 298 K.

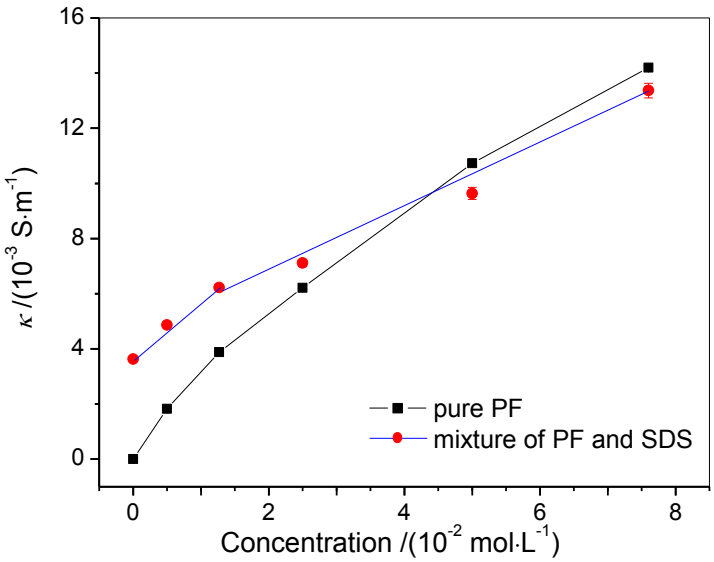

Fig. S1 The κ values of the solutions of PF in the absence and presence of SDS (C_{SDS}, 8.68×10^{-2} mol dm^{-3}; C_{PF}, 0~ 7.60×10^{-2} mol dm^{-3}). The κ was calculated as an average of three repeated measurements at 293 K.

Fig. S2 The transparent solution obtained in the hydrothermal porcesses of PF (5.00×10^{-3} mol dm^{-3}) in the presence of SDS (8.68×10^{-2} mol dm^{-3}).

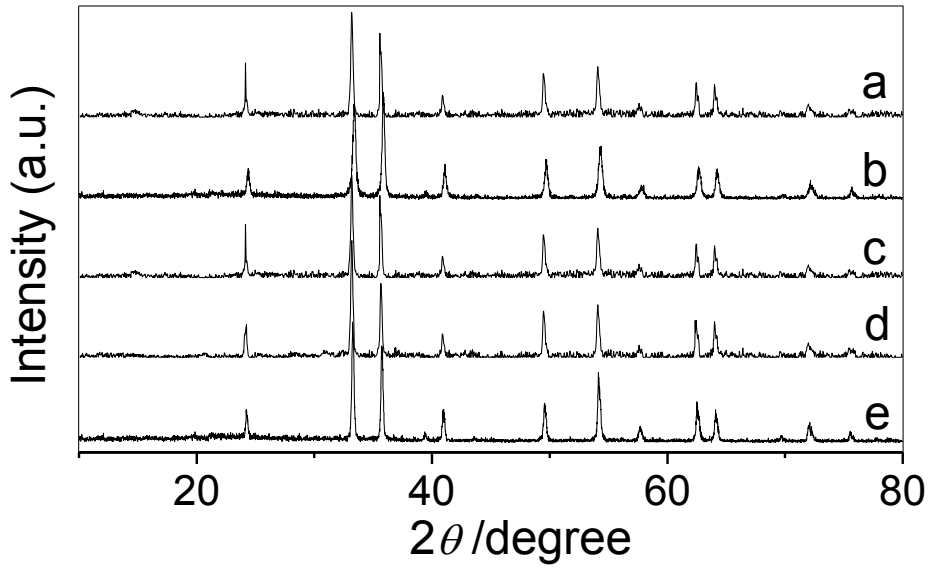

Fig. S3 Powder XRD patterns of the Fe_2O_3 obtained in the hydrothermal porcesses of PF (2.50×10^{-2} mol dm^{-3}) in the presence of *n*-octane (a), hexadecyl trimethyl ammonium bromide (b), sodium dodecylbenzenesulfonate (c), sodium sulfate (d) and sodium sulfite (e) with the concentration of 8.68×10^{-2} mol dm^{-3}.

The thermogravimetric and differential thermogravimetric profiles (Figure S4) of the crystal tubes in air show a two-step degradation process. The first degradation occurred at 445 K with a weight loss of 19.3%, corresponding to the release of two water molecules, which agrees well with the calculated value of 19.0% in IOD. The second degradation occurred at 657 K with a final residual mass of 46.6% due to the Fe_2O_3 (calculated value of 46.5%) resulted from the oxidation of IOD. [1]

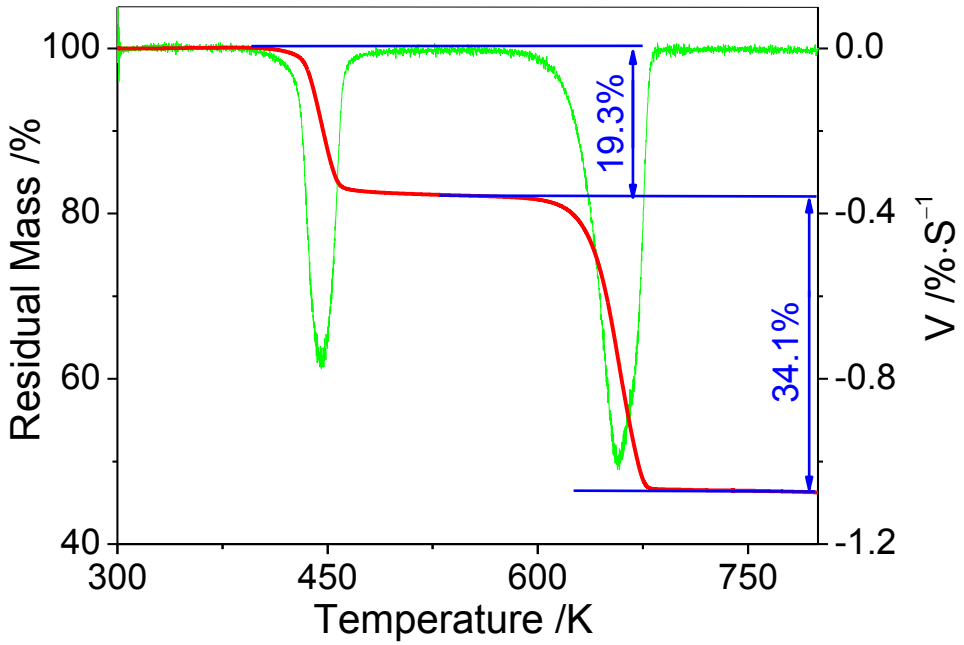

Fig. S4 The TG and DTG profiles of the IOD-1 crystals.

1 a) M. Hermanek, R. Zboril, M. Mashlan, L. Machala, O. Schneeweiss, *J. Mater. Chem.*, 2006, **16**, 1273. b) C. Cavelius, K. Moh, S. Mathur, *Cryst. Growth. Des.*, 2012, **12**, 5948. c) Z. Dang, L. X. Song, J. Yang, J. Chen, Y., Teng, *Dalton T.*, 2012, **41**, 3006.

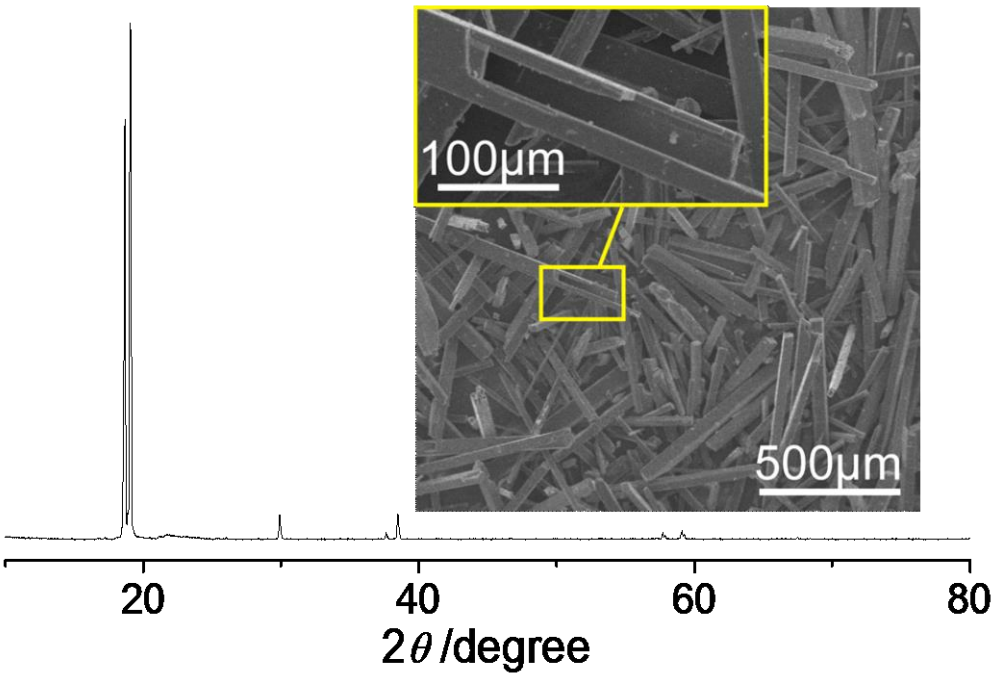

Fig. S5 The powder XRD pattern and SEM image of IOD-3 obtained in the hydrothermal processes of PF (2.50×10^{-2} mol dm^{-3}) in the presence of SDS (5.00×10^{-2} mol dm^{-3}). The yellow boxes exhibit the magnified SEM image of one tube.

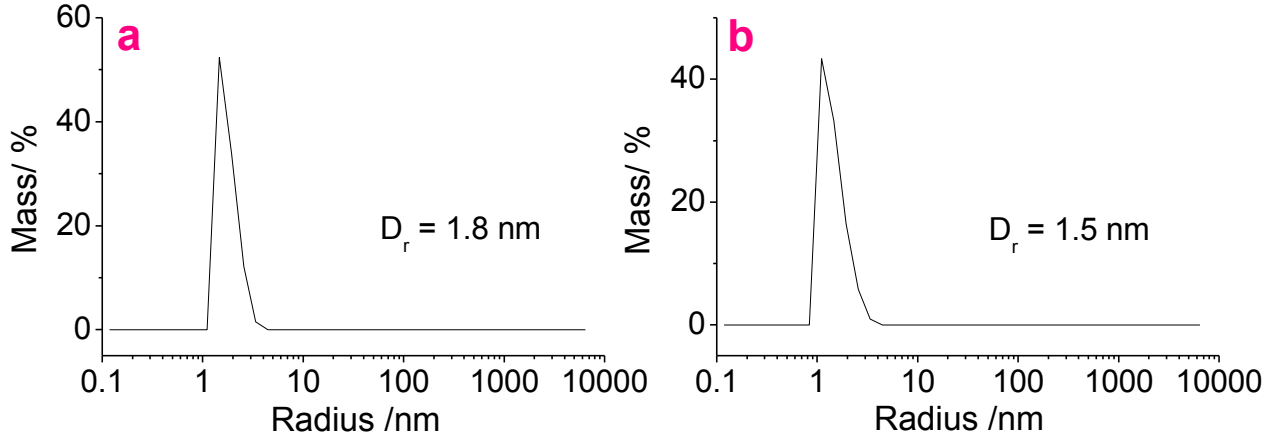

Fig. S6 DLS curves of the PF-SDS-SM in the solutions of SDS (8.68×10^{-2} mol dm^{-3}) in the presence of PF (2.50×10^{-2} mol dm^{-3}, a; and 5.00×10^{-2} mol dm^{-3}, b).

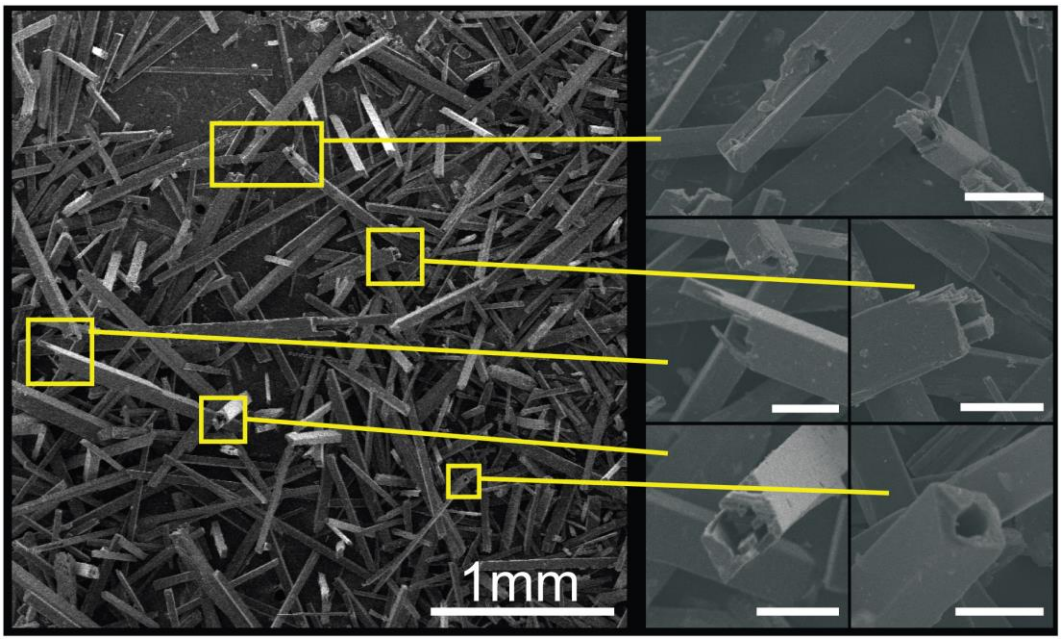

Fig. S7 SEM image of the IOD-1 before removal of SDS micelles. The yellow boxes exhibit magnified cross sections of the tubes. The white bars in the right column refer to 100 μm.